Thermochimica Acta 515 (2011) 32–37

Contents lists available at ScienceDirect

Thermochimica Acta

journal homepage: www.elsevier.com/locate/tca

Synthesis and curing kinetics of benzoxazine containing fluorene and furan groups

Yanbing Lu*, Mingming Li, Yingjun Zhang, Ding Hu, Lili Ke, Weijian Xu

Institute of Polymer Science and Engineering, College of Chemistry & Chemical Engineering, Hunan University, Changsha 410082, China

ARTICLE INFO

Article history:
Received 29 August 2010
Received in revised form 2 December 2010
Accepted 15 December 2010
Available online 29 December 2010

Keywords:
Benzoxazine
Curing kinetics
Fluorene
Furan
Autocatalytic curing

ABSTRACT

A novel benzoxazine bearing fluorene and furan group (B-bff) was prepared using 9,9-bis(4-hydroxyphenyl) fluorene, furfurylamine and formaldehyde as raw materials. The chemical structure of B-bff was characterized with FTIR, ^{1}H NMR, ^{13}C NMR, and elemental analysis. The curing reaction was investigated under non-isothermal differential scanning calorimetry (DSC) at different heating rates. The apparent activation energy of the curing reaction was determined to be 119.1 kJ mol^{-1} and 121.3 kJ mol^{-1}, respectively, according to Kissinger and Ozawa method. Isoconversional analysis of the DSC data showed that the activation energy value decreased with the degree of conversion. The autocatalytic kinetic model was found to be the best description of the investigated curing reactions. In addition, the predicted curves from our kinetic models fit well with the non-isothermal DSC thermograms. Thermogravimetric analysis (TGA) result showed that the cured polymer possessed good thermal properties with the 5% weight loss temperature 402 °C and char yield at 900 °C 57%.

© 2010 Elsevier B.V. All rights reserved.

1. Introduction

Over the past several years, the applications for high temperature resistant polymers have increased drastically due to technological advancements. Polybenzoxazine, as a novel type of phenolic resins, have drawn worldwide attention because they overcome many of the deficiencies commonly associated with novolac and resol-type phenolic resins. They have demonstrated various attractive properties including high thermal stability, high char yields, high glass transition temperature (T_g), near-zero volumetric change upon curing, good mechanical and dielectric properties, low water absorption, and low flammability [1–8]. These characteristics make benzoxazine polymers excellent candidates for high performance composites. The chemistry for the synthesis of the benzoxazine deals with Mannich reaction involving the condensation of phenol, formaldehyde, and primary amine. The wide variety of available phenolic derivatives and primary amines allow for tremendous opportunities in molecular design. By taking of the molecular design flexibility of benzoxazine chemistry, thermal and thermo-oxidative stabilities of benzoxazine have been improved [9–25].

Fluorene-based polymers show a number of interesting and unique chemical and physical properties, such as good heat resistance, high char yield, high limited oxygen index, good flame retardant, and excellent solubility in common organic solvents [26–28]. Introduction of the stiff, bulky cardo moieties into benzoxazine can enhance the rigidity and thermal stability of the final product. Wang et al. synthesized benzoxazines from bisphenolic fluorene, formaldehyde and aniline [29]. The obtained resin showed good thermal properties. In this study, by taking advantage of the high flexibility in molecular design of benzoxazine, we prepared a novel flourene-based benzoxazine from bisphenolic flourene, formaldehyde and furfurylamine. Compared with other amine derivative, furfurylamine's advantages are: (a) incorporation of furan groups to benzoxazines so as to simplify polymerization reactions, (b) formation of linkages between Mannich bridges and aromatic furan groups during polymerization to increase the cross-linking densities of the resulting polymers, and further enhance the glass transition temperatures and thermal stability, (c) char-formation enrichment with furan groups, and (d) using economic and ecological furan compound as a raw material in synthesis [30]. The structure of the prepared benzoxazine is confirmed by FTIR, ^{1}H and ^{13}C NMR and elemental analysis. Curing behavior of the obtained benzoxazine monomer and thermal properties of cured polymer are also investigated.

2. Experimental

2.1. Materials

9,9-Bis(4-hydroxyphenyl) fluorene (BHPF) was purchased from Suqian Ever-Galaxy Pharmacy & Chem. Co., China. Fur-

* Corresponding author. Tel.: +86 731 88823112; fax: +86 731 88822863.
E-mail address: yanbinglu@hnu.cn (Y. Lu).

0040-6031/$ – see front matter © 2010 Elsevier B.V. All rights reserved.
doi:10.1016/j.tca.2010.12.014

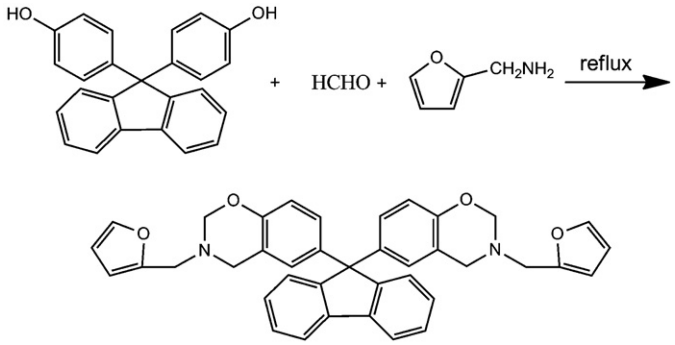

Scheme 1.

furylamine was purchased from Aladding Reagent Company. Dichloromethane, ethanol, 1,4-dioxane, sodium hydrate, diethyl ether, and formaldehyde were purchased from Tianjin Fuchen Chemical Reagent Factory. All chemicals were used as received.

2.2. Monomer synthesis

The benzoxazine monomer B-bff (Scheme 1) was synthesized according to the method reported by Wang et al. [29] with some essential modifications.

Formaldehyde (2.64 g, 0.088 mol) and 1,4-dioxane (20 mL) were added to a 250 mL three neck round-bottomed flask equipped with a magnetic stirrer, reflux condenser, stirred 20 min at room temperature. The mixture was cooled to below 5 °C in an ice bath, then furfurylamine (3.88 g, 0.04 mol) was added drop-wise and reacted for 1 h. Then, a solution of BHPF (7 g, 0.02 mol) in 20 mL mixed solvents including dioxane (10 mL) and ethanol (10 mL) as a cosolvent to improve the solubility of BHPF was added. The temperature was raised gradually to 100 °C and the mixture was kept stirring for 12 h. The solvent was removed by rotary evaporator. The yellowish powder was dissolved in chloroform, washed three times with 2 mol L^{-1} NaOH aqueous solution and finally two times with distilled water. The chloroform phase was collected dried with anhydrous sodium sulphate. Crude product obtained from removing the solvent was re-crystallized from diethyl ether to give the final product: 65% yield.

2.3. Characterization

Fourier transform infrared (FTIR) spectrum was performed on a WQF-410 spectrophotometer (Beijing Second Optical Instrument Factory). Proton nuclear magnetic resonance (^{1}H NMR) spectrum was recorded on an INOVA-400 instrument (Varian, United States). Elemental analyses were obtained from Heraeus CHN-rapid elemental analyzer.

DSC and TGA measurements were performed on a Netzsch STA 409 (Netzsch, Germany) under nitrogen atmosphere. The instrument was calibrated with a high purity indium standard, and an empty cell was used as the reference. About 10 mg of sample was weighed into a hermetic aluminum sample pan at room temperature, which was then sealed, and the sample was tested immediately. The curing thermal date were obtained with different heating rates (2, 5, 10, 15 and 20 °C min^{-1}), heated from 30 to 400 °C. The heat flow data, as a function of temperature and time, were obtained using the area under the peak of the exotherm. These data were processed further to obtain the fractional conversion and the rate of reaction.

3. Results and discussion

3.1. Preparation and characterization of B-bff

The benzoxazine monomer was prepared from BHPF, furfurylamine and formaldehyde via a solution method. Because of the poor solubility of BHPF in nonpolar solvents such as 1,4-dioxane or chloroform, the mixed solvents of 1,4-dioxane and ethanol were used in the reaction process. Ishida and co-workers have verified that nonpolar solvents, for example, chloroform carbon tetrachloride, dioxane, or *n*-hexane, help ring closure of the open Mannich base, and reduce the chances of ring opening [25]. In this work, the yield of B-bff monomers is about 65% while the volume ratio of ethanol and 1,4-dioxane is 1:1. The reasons may be attributed to the disadvantageous effect of polar solvent and great steric hindrance of bulky fluorenyl group on the formation of oxazine ring.

The chemical structure of B-bff was confirmed with FTIR, ^{1}H NMR, ^{13}C NMR, and element analysis. Fig. 1 shows the FTIR spectrum of the obtained benzoxazine compound. The oxazine ring was observed with the characteristic absorptions at 1230 cm^{-1} (asymmetric stretching of C–O–C), 1014 cm^{-1} (symmetric stretching of C–O–C), 1117 cm^{-1} (asymmetric stretching of C–N–C), and 866 cm^{-1} (C–N–C symmetric stretching), indicating that monomer containing benzoxazine structure is obtained [29,31,32]. The furan group was observed with the absorption peaks at 1585, 985, and 763 cm^{-1} [30].

The ^{1}H and ^{13}C NMR spectra were also measured to confirm the structure. Fig. 2 shows the ^{1}H NMR spectrum of B-bff. The furan ring was characterized with the absorption peaks at 6.20–6.31 ppm (═CH–CH═) and at 7.38 ppm (–CH═CH–O–). The furan ring protons were observed at 6.20–7.76 ppm. The absorption peaks of aromatic protons appeared at 6.65–7.30 ppm. The characteristic peaks assigned to methylene (O–CH_2–N) and methylene (Ar–CH_2–C) of oxazine ring for the benxoxazine appeared at 4.81 and 3.88 ppm, respectively, confirming the formation of benzoxazine monomer [29,33–35]. The single peak at 3.87 ppm associated with the absorption of protons of –CH_2N– in furfuryl groups.

In the corresponding ^{13}C NMR spectrum in Fig. 3, the resonances at 40–90 and 110–160 ppm were assigned to the methylene carbons, and the aromatic carbons, respectively [29]. The chemical shifts located at 81.6 and 49.8 ppm were attributed to the carbon atom resonances of O–CH_2–N and Ar–CH_2–N of oxazine rings, respectively. The characteristic peaks of the carbon atom of –CH_2N–

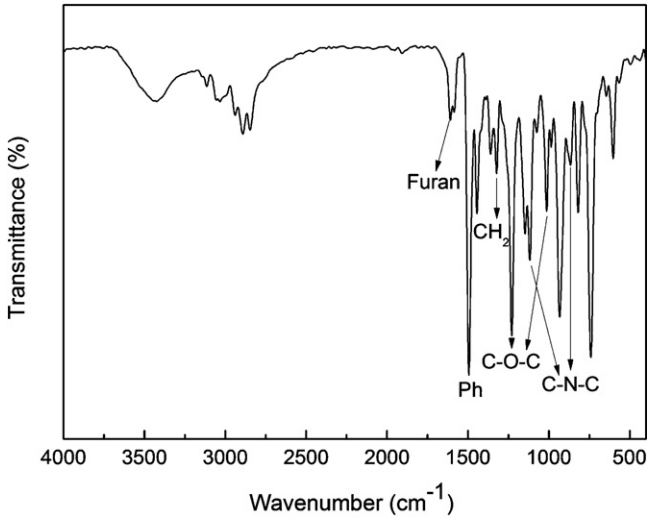

Fig. 1. FTIR spectrum of benzoxazine B-bff.

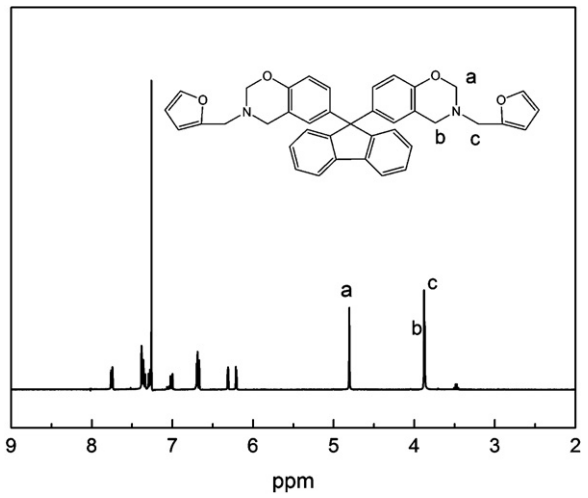

Fig. 2. ^{1}H NMR spectrum of benzoxazine B-bff.

in furfuryl group located at 49.8 ppm. The peak at 64.3 ppm was assigned to the quaternary carbon atom of fluorene ring.

The purity of the obtained benzoxazine was verified with the elemental analysis data. The data shows that the experimental results (C, 78.86; H, 5.41 and N, 4.84) are in reasonable agreement with the calculated value (C, 79.03; H, 5.44 and N, 4.73).

3.2. Curing behavior of B-bff

The curing behavior of the novel fluorine containing benzoxazine B-bff was studied by DSC. Fig. 4 shows a typical example of the DSC thermogram for B-bff recorded at 10 °C min^{-1}. As can be seen in Fig. 4, the endothermal peak at about 178 °C was assigned to the melting of the benzoxazine and the exothermal peak in the temperature range between 200 and 300 °C was assigned to the curing reaction of B-bff.

Figs. 5 and 6 show the DSC thermogram of B-bff and the conversion versus temperature at different heating rates. From Fig. 5, information about the nature of the curing reaction such as initial curing temperature (T_i), peak temperature (T_p), and the curing range at different heating rates could be derived. The data obtained are summarized in Table 1. It can be observed that the increase of heating rate leads to decrease of the cure time, and the exothermic peak shifts to a higher temperature with higher heating rate.

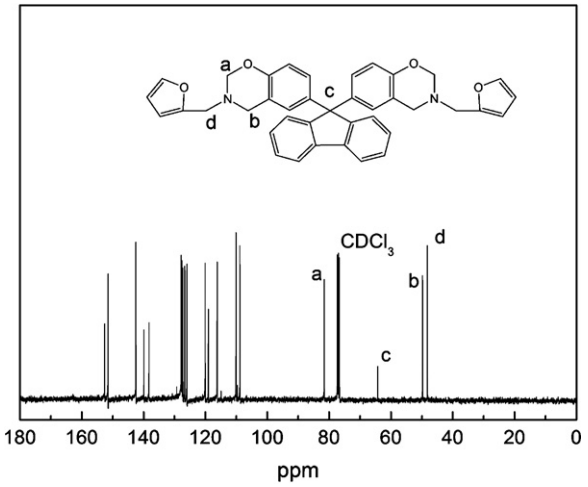

Fig. 3. ^{13}C NMR spectrum of benzoxazine B-bff.

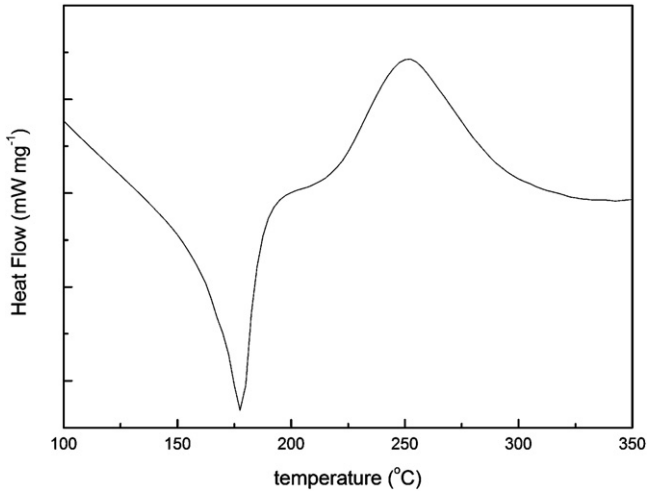

Fig. 4. A typical DSC curve of B-bff at a heating rate of 10 °C min^{-1}.

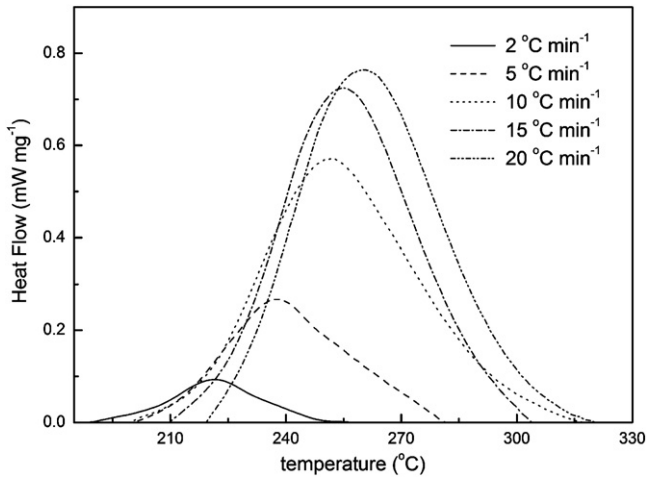

Fig. 5. DSC curves of B-bff at different heating rates.

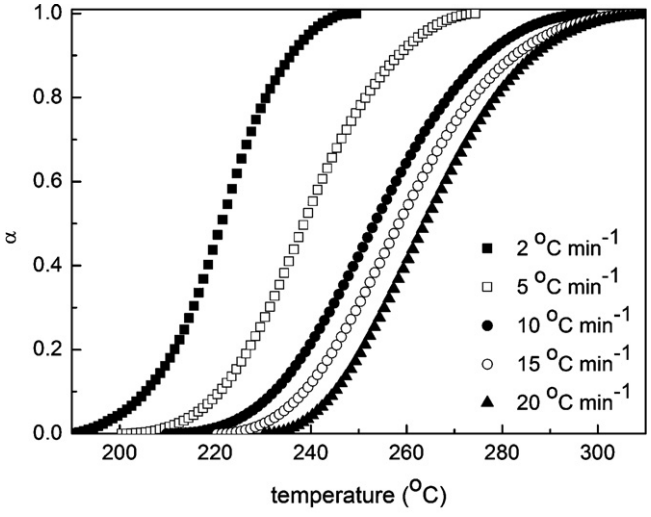

Fig. 6. Conversion as a function of cure temperature for B-bff at different heating rates.

Table 1
Curing characteristics of B-bff at various heating rate.

Heating rate (°C min^{-1})	T_i	T_p	T_f	Cure time (min)
2	183.4	222.5	256.7	36
5	198.2	237.4	281.3	17
10	204.7	251.8	305.4	10
15	211.8	255.4	315.7	7
20	220.1	262.3	320.4	5

Generally, the apparent activation energy E_a can be calculated by using the well-known methods for dynamic heating experiment, Kissinger method and Ozawa method [36,37].

Kissinger method is based on the fact that exothermic peak temperature T_p varies with the heating rates and it assumes that the maximum reaction rate occurs at the peak temperatures. The equation can be expressed as Eq. (1):

$$\ln \frac{\beta}{T_p^2} = \ln\left(\frac{AR}{E_a}\right) - \frac{E_a}{RT_p} \quad (1)$$

where β is the heating rate, A the frequency factor, and R the universal gas constant.

If the plot of $\ln(\beta/T_p^2)$ against $1/T_p$ is linear, the E_a can be obtained from the slope of the corresponding straight line. Fig. 7 shows the plot of $\ln(\beta/T_p^2)$ against $1/T_p$ for B-bff. The E_a value of 119.1 kJ mol^{-1} was estimated.

Another theoretical treatment, namely, the Ozawa method can be also applied to the thermal data, using the following Eq. (2):

$$\ln \beta = -5.331 - 1.052\left(\frac{E_a}{RT_p}\right) + \ln\left(\frac{AE_a}{R}\right) - \ln f(\alpha) \quad (2)$$

It's on the assumption that the degree of conversion at peak temperatures for different heating rates is constant. Thus, at the same conversion, the plot of ln β versus $1/T_p$, as shown in Fig. 7, should be a straight line with the slope of 1.052 E_a/R. The E_a value calculated was 123.1 kJ mol^{-1}. The E_a values from Kissinger and Ozawa method are quite close to each other and their differences may be caused by the different of assumptions.

However, in most benzoxazine curing process, both the activation energy and pre-exponential factor are functions of the cure. In order to find the E_a dependency for the B-bff cure process, the advanced isoconversional method developed by Vyazovkin [38–42] was used. For a set of n experiments carried out at different heating

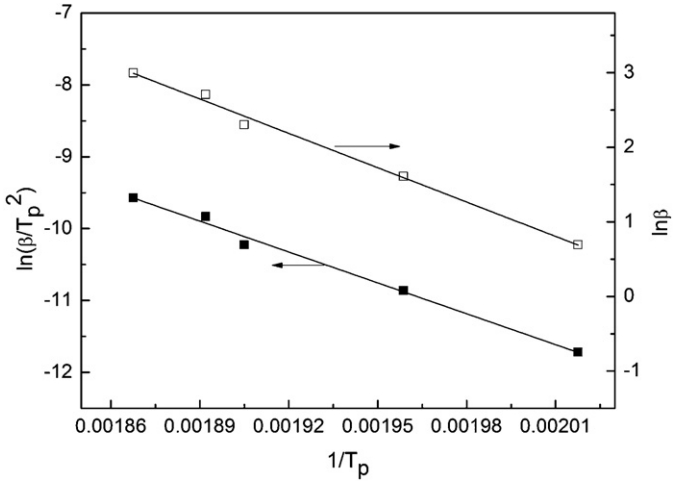

Fig. 7. Representations of Kissinger and Ozawa methods to calculation activation energy from non-isothermal date for the benzoxazine monomer.

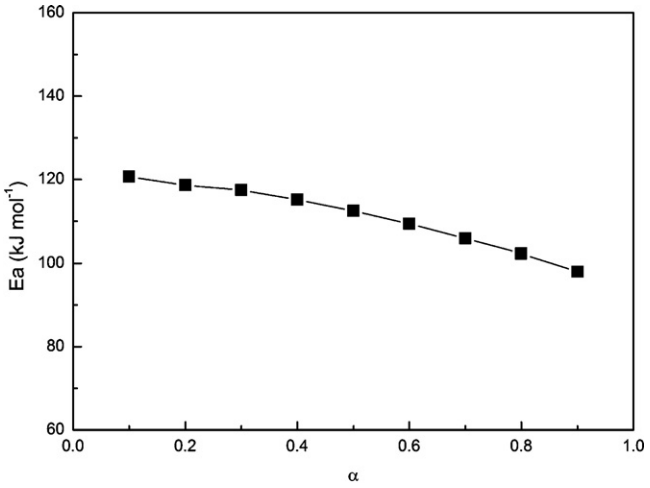

Fig. 8. Variation of E_a versus conversion.

rates, the activation energy is determined at any particular value of α by finding the value of E_a that minimizes the function

$$\phi(E_\alpha) = \sum_{i=1}^{n}\sum_{j\neq 1}^{n} \frac{J[E_\alpha, T_i(t_\alpha)]}{J[E_\alpha, T_j(t_\alpha)]} \quad (3)$$

In Eq. (3), the integral

$$J\left[E_\alpha, T_i(t_\alpha) = \int_0^{t_\alpha} \exp\left[-\frac{E_\alpha}{RT_i(t)}\right] dt\right] \quad (4)$$

is evaluated numerically for a set of experimental heating processes. The minimization procedure is repeated for each value of α to determine the E_a dependence. Fig. 8 presents activation energy as a function of conversion. It can be seen that the activation energy values tend to decrease with the degree of conversion.

3.3. Curing kinetic model

To examine the kinetic model, it is necessary to appeal to the special functions $y(\alpha)$ and $z(\alpha)$ [43,44].

$$y(\alpha) = \left(\frac{d\alpha}{dt}\right) e^x \quad (5)$$

$$z(\alpha) = \pi(x)\left(\frac{d\alpha}{dt}\right)\frac{T}{\beta} \quad (6)$$

where x is reduced activation energy (E_a/RT), β the heating rate, T absolute temperature and $\pi(x)$ is the expression of the temperature integral. In our study, the activation energy value obtained from Kissinger method was used. As was pointed out, $\pi(x)$ function can be well approximated using the 4th rational expression of Senum and Yang [45] as in Eq. (7)

$$\pi(x) = \frac{x^3 + 18x^2 + 88x + 96}{x^4 + 20x^3 + 120x^2 + 240x + 120} \quad (7)$$

For practical reasons, the $y(\alpha)$ and $z(\alpha)$ functions are normalized within (0, 1) range. Figs. 9 and 10 show the variation of $y(\alpha)$ and $z(\alpha)$ values with conversion. These functions exhibit maxima at α_M and α_p^∞, respectively. Both α_M and α_p^∞ help to decide the choice of the kinetic model [43,44].

Table 2 lists the values of maxima α_M and α_p^∞ corresponding to the functions $y(\alpha)$ and $z(\alpha)$, together with α_p taken as the maximum of the DSC peak. It can be seen that α_M, α_p^∞ and α_p values were independent with the heating rate. And the values of α_M were lower against the value of α_p, while α_p^∞ exhibits values lower than 0.632 (a characteristic value for the kinetic model determination) [46]. These remarks indicate that the studied curing process can

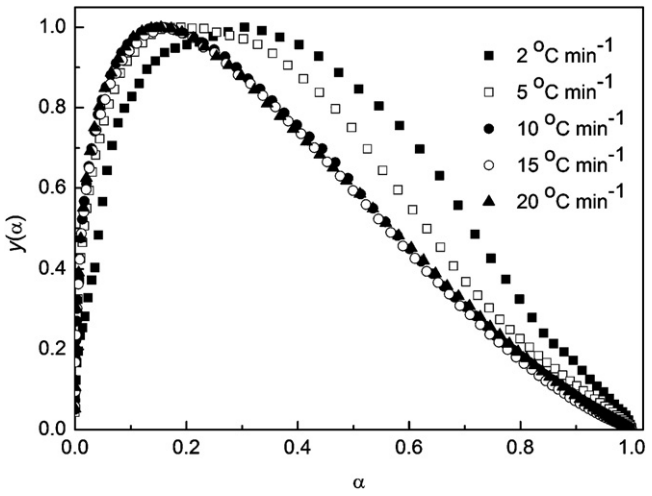

Fig. 9. Variation of $y(\alpha)$ function versus conversion at different heating rates.

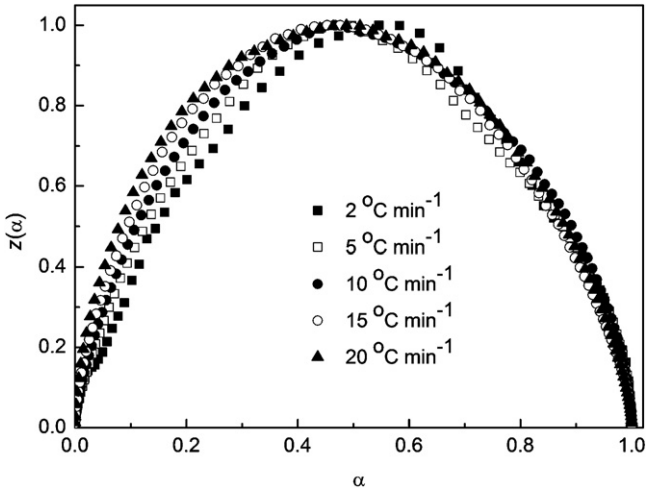

Fig. 10. Variation of $z(\alpha)$ function versus conversion at different heating rates.

be described using the two parameter autocatalytic kinetic model Šesták–Berggren (Eq. (8)) [47].

$$f(\alpha) = (1-\alpha)^n \alpha^n \tag{8}$$

where m and n are the kinetic exponents.

Thus, the reaction rate can be described as follows:

$$\frac{d\alpha}{dT} = \frac{A}{\beta}\exp(-\frac{E_a}{RT})(1-\alpha)^n \alpha^m \tag{9}$$

Theoretically, Eq. (9) could be solved by multiple nonlinear regressions because the curing rate is an exponential function of the reciprocal of the absolute temperature. By taking the natural logarithm of Eq. (9), a linear expression for the natural logarithm of curing rate can be obtained:

$$\ln(\beta\frac{d\alpha}{dT}) = \frac{E_a}{RT} + n \quad \ln(1-\alpha) + m \quad \ln(a) + \ln A \tag{10}$$

Eq. (10) can be solved by multiple linear regression, in which the dependent variable is $\ln(d\alpha/dt)$, and the independent variables are $1/T$, $\ln(1\text{-}\alpha)$ and $\ln(\alpha)$. Therefore, the values of A, m, and n can be obtained using the average activation energy from Kissinger method. The degree of curing is chosen between the beginning of the reaction and the maximum peak of degree of curing (α = 0.1–0.5). The kinetic parameters evaluated for the proposed Šesták–Berggren kinetic model were listed in Table 3.

The correctness of the kinetic model proposed using the Šesták–Berggren equation was verified. The experimental curves and calculated curves at different heating rates are shown in Fig. 11. It is clearly seen that the calculated data from the model are in good agreement with the experimental results. This means that the two parameter Šesták–Berggren model gives a good description of the curing process.

Table 2
The values of α_p, α_M and α_p^∞ obtained from DSCthermograms analysis.

Heating rate (°C min^{-1})	α_p	α_M	α_p^∞
2	0.55	0.30	0.55
5	0.47	0.19	0.47
10	0.47	0.15	0.47
15	0.43	0.16	0.45
20	0.46	0.15	0.49

Table 3
The kinetic parameters evaluated for the B-bff.

Heating rate (°C min^{-1})	E (kJ mol^{-1})	ln A (s^{-1})	Mean	n	Mean	m	Mean
2	119.1	27.4	27.2	1.01	1.40	0.47	0.32
5		27.1		1.25		0.33	
10		27.0		1.53		0.26	
15		27.2		1.64		0.29	
20		27.2		1.55		0.25	

3.4. Thermal properties

The thermal stability of benzoxazine was estimated by the thermogravimetric analysis under nitrogen atmosphere. The char yield, as defined as the weight residue remaining at 900 °C under nitrogen atmosphere, was 57%, reflecting that the prepared benzoxazine resin has the excellent thermal stability. The 5 and 10% weight loss temperatures (T_5 and T_{10}) were 402 and 422 °C, respectively. However, the T_5 and T_{10} values of benzoxazine synthesized from 9,9-bis(4-hydroxyphenyl) fluorene and aniline were about 334 and 364 °C, respectively [29], and those of benzoxazine synthesized from bisphenol-A and furfurylamine about 347 and 391 °C, respectively [30]. The higher T_5 and T_{10} values showed that the introduction of rigid fluorene skeleton with bulky pendent

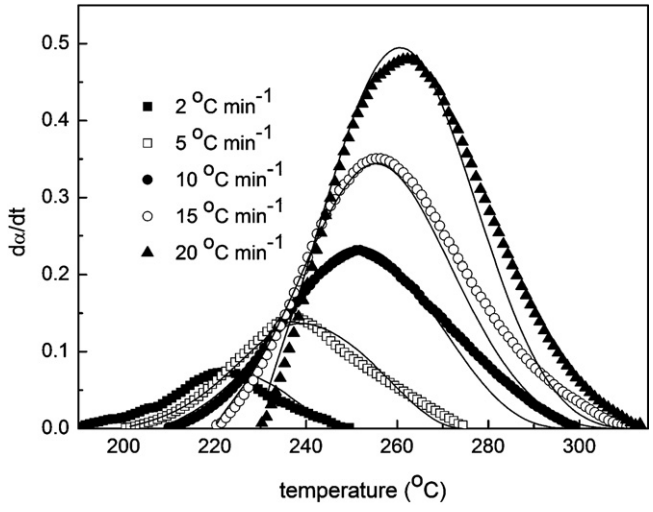

Fig. 11. Experimental (symbols) and calculated (solid lines) DSC peaks corresponding to the curing process of benzoxazine monomer.

cardo moieties and crosslinkable furan group into benzoxazine monomers can improve the inherent thermal stability of the thermosets dramatically.

4. Conclusion

9,9-Bis(4-hydroxyphenyl) fluorene based benzoxazine monomer B-bff was prepared with a solution method and its structure was confirmed by FTIR and ^{1}H NMR. The curing kinetics of B-bff was investigated via non-isothermal DSC. The activation energy by Kissinger's and Ozawa's method were 119.1 and 121.3 kJ mol^{-1}, respectively. Isoconversional analysis of the DSC data revealed that the activation energy decreased with the degree of cure. The autocatalytic kinetic model was found to be the best description of the investigated curing reactions. Evidently, the kinetic model of the curing reaction of B-bff is in good agreement with non-isothermal DSC results. TGA result shows that the prepared benzoxazine has the excellent thermal stability.

Acknowledgement

The authors gratefully acknowledge the financial support by the Natural Science Foundation of Hunan Province, China (Grant no. 09JJ5009).

References

[1] X. Ning, H. Ishida, J. Polym. Sci. Part A: Polym. Chem. 32 (1994) 921–928.
[2] N.N. Ghosh, B. Kiskan, Y. Yagci, Prog. Polym. Sci. 32 (2007) 1344–1391.
[3] A. Laobuthee, S. Chirachanchai, H. Ishida, K. Tashiro, J. Am. Chem. Soc. 123 (2001) 9947–9955.
[4] C.P. Reghunadhan Nair, Prog. Polym. Sci. 29 (2004) 401–498.
[5] H. Ishida, D.J. Allen, J. Polym. Sci. Part B: Polym. Phys. 34 (1996) 1019–1030.
[6] S.B. Shen, H. Ishida, J. Polym. Sci. Part B: Polym. Phys. 37 (1999) 3257–3268.
[7] H. Ishida, D.P. Sanders, Macromolecules 33 (2000) 8149–8157.
[8] H.L. Zhong, Y.B. Lu, J.R. Chen, W.J. Xu, X. Liu, J. Appl. Polym. Sci. 118 (2010) 705–710.
[9] C.H. Lin, S.L. Chang, T.P. Wei, S.H. Ding, W.C. Su, Polym. Degrad. Stab. 95 (2010) 1167–1176.
[10] T. Agag, L. Jin, H. Ishida, Polymer 50 (2009) 5940–5944.
[11] Y.F. Liu, Z.Q. Yue, J.G. Gao, Polymer 51 (2010) 3722–3729.
[12] J.X. Huang, J. Zhang, F. Wang, F.R. Huang, L. Du, React. Funct. Polym. 66 (2006) 1395–1403.
[13] D.J. Allen, H. Ishida, Polymer 50 (2009) 613–626.
[14] S. Tiptipakorn, S. Damrongsakkul, S. Ando, K. Hemvichian, S. Rimdusit, Polym. Degrad. Stab. 92 (2007) 1265–1278.
[15] L. Wang, S.X. Zheng, Polymer 51 (2010) 1124–1132.
[16] H. Ishida, H.Y. Low, Macromolecules 30 (1997) 1099–1106.
[17] H. Ishida, Y. Rodriguez, Polymer 36 (1995) 3151–3158.
[18] R. Rimdusit, H. Ishida, Polymer 41 (2000) 7941–7949.
[19] H.D. Kim, H. Ishida, Macromolecules 36 (2003) 8320–8329.
[20] C. Jubsilp, K. Punson, T. Takeichi, S. Rimdusit, Polym. Degrad. Stab. 95 (2010) 918–924.
[21] D.R. Yei, H.K. Fu, W.Y. Chen, F.C. Chang, J. Polym. Sci. Part B: Polym. Phys. 44 (2006) 347–358.
[22] K.S. Santhosh Kumar, C.P. Reghunadhan Nair, R. Sadhana, K.N. Ninan, Eur. Polym. J. 43 (2007) 5084–5096.
[23] Z.X. Shi, D.S. Yu, Y.Z. Wang, R.W. Xu, J. Appl. Polym. Sci. 88 (2003) 194–200.
[24] C. Jubsilp, S. Damrongsakku, T. Takeichi, S. Rimdusit, Thermochim. Acta 447 (2006) 131–140.
[25] H. Ishida, H.Y. Low, J. Appl. Polym. Sci. 69 (1998) 2559–2567.
[26] N. Biolley, M. Grágoire, T. Pascal, B. Sillion, Polymer 32 (1991) 3256–3261.
[27] G.Z. Yang, M. Wu, S. Lu, M. Wang, T.X. Liu, W. Huang, Polymer 47 (2006) 4816–4823.
[28] Y. Zhang, Z. Huang, W.J. Zeng, Y. Cao, Polymer 49 (2008) 1211–1219.
[29] J. Wang, M.Q. Wu, W.B. Liu, S.W. Yang, J.W. Bai, Q.Q. Ding, Y. Li, Eur. Polym. J. 46 (2010) 1024–1031.
[30] Y.L. Liu, C. Chou, J. Polym. Sci. Part A: Polym. Chem. 43 (2005) 5267–5282.
[31] J. Dunkers, H. Ishida, Spectrochim. Acta 51A (1995) 855–867.
[32] J. Dunkers, H. Ishida, Spectrochim. Acta 51A (1995) 1061–1074.
[33] H. Ishida, S. Ohba, Polymer 46 (2005) 5588–5595.
[34] T. Agag, T. Takeichi, J. Polym. Sci. Part A: Polym. Chem. 44 (2006) 1424–1435.
[35] Y.L. Liu, J.M. Yu, C. Chou, J. Polym. Sci. Part A: Polym. Chem. 42 (2004) 5954–5963.
[36] H.E. Kissinger, Anal. Chem. 29 (1957) 1702–1706.
[37] T. Ozawa, J. Thermal Anal. 2 (1970) 301–324.
[38] N. Sbirrazzuoli, S. Vyazovkin, Thermochim. Acta 388 (2002) 289–298.
[39] S. Vyazovkin, J. Comput. Chem. 18 (1997) 393–402.
[40] S. Vyazovkin, J. Comput. Chem. 22 (2001) 178–183.
[41] S. Vyazovkin, N. Sbirrazzuoli, Macromol. Rapid Commun. 27 (2006) 1515–1532.
[42] S. Vyazovkin, N. Sbirrazzuoli, Macromol. Chem. Phys. 200 (1999) 2294–2303.
[43] J. Malek, Thermochim. Acta 355 (2000) 239–253.
[44] J. Malek, Thermochim. Acta 200 (1992) 257–269.
[45] G.I. Senum, R.T. Yang, J. Thermal. Anal. 11 (1977) 445–447.
[46] S. Montserrat, J. Malek, Thermochim. Acta 228 (1993) 47–60.
[47] C. Šesták, G. Berggren, Thermochim. Acta 3 (1971) 1–12.